Improved terahertz two-color plasma sources pumped by high intensity laser beam

F. Blanchard, G. Sharma, X. Ropagnol, L. Razzari*, R. Morandotti and T. Ozaki

INRS-EMT, Advanced Laser Light Source, Université du Québec, Varennes, Québec J3X 1S2, Canada
*also with : Dipartimento di Elettronica, Università di Pavia, via Ferrata 1, Pavia 27100, Italy
blanchard@emt.inrs.ca

Abstract: We investigate the intensity dependent spatial drift of two-color plasma based terahertz (THz) sources. A simple scheme that uses an off-axis parabolic mirror is presented to overcome this shifting. In addition, the THz energy and electric field measurements are related via the real time images of the THz spot size.

OCIS codes: (260.5210) Photoionization; (300.6270) Spectroscopy, far infrared; (320.7120) Ultrafast phenomena; (350.5400) Plasmas.

References and links

1. M. C. Nuss and J. Orenstein, *Terahertz Time-Domain Spectroscopy*, Millimeter and Submillimeter Wave Spectroscopy of Solids, G. Grüner, ed., (Springer, Berlin, 1998).
2. D. Mittleman, *Sensing with Terahertz Radiation*, (Springer-Verlag, Berlin, 2003).
3. B. Ferguson and X.-C. Zhang, "Materials for terahertz science and technology," Nat. Mater. **1**, 26-33 (2002).
4. A. G. Stepanov, L. Bonacina, S. V. Chekalin, and J. –P. Wolf, "Generation of 30 μJ single-cycle terahertz pulses at 100 Hz repetition rate by optical rectification," Opt. Lett. **33**, 2497-2499 (2008).
5. J. Hebling, G. Almási, and I. Z. Kozma "Velocity matching by pulse front tilting for large area THz-pulse generation," Opt. Express **10**, 1161-1166 (2002).
6. H. Hamster, A. Sullivan, S. Gordon, W. White, and R. W. Falcone, "Subpicosecond, electromagnetic pulses from intense laser-plasma interaction," Phys. Rev. Lett. **71**, 2725-2728 (1993).
7. D. J. Cook and R. M. Hochstrasser, "Intense terahertz pulses by four-wave rectification in air," Opt. Lett. **25**, 1210-1212 (2000).
8. M. Kress, T. Löffler, S. Eden, M. Thomson, and H. G. Roskos, "Terahertz-pulse generation by photoionization of air with laser pulses composed of both fundamental and second-harmonic waves," Opt. Lett. **29**, 1120-1122 (2004).
9. T. Bartel, P. Gaal, K. Reimann, M. Woerner, and T. Elsaesser, "Generation of single-cycle THz transients with high electric-field amplitudes," Opt. Lett. **30**, 2805-2807 (2005).
10. X. Xie, J. Dai, and X.-C. Zhang, "Coherent control of THz wave generation in ambient air," Phys. Rev. Lett. **96**, 075005(2006).
11. K. Y. Kim, J. H. Glownia, A. J. Taylor, and G. Rodriguez, "Terahertz emission from ultrafast ionizing air in symmetry-broken laser fields," Opt. Express **15**, 4577-4584 (2007).
12. K. Y. Kim, A. J. Taylor, J. H. Glownia, and G. Rodriguez, "Coherent control of terahertz supercontinuum generation in ultrafast laser–gas interactions," Nature Photon. **2**, 605-609 (2008).
13. http://www.alls.ca/
14. S. Fourmaux, S. Payeur, A. Alexandrov, C. Serbanescu, F. Martin, T. Ozaki, A. Kudryashov, and J. C. Kieffer, "Laser beam wavefront correction for ultra-high intensities with the 200 TW laser system at the Advanced Laser Light Source," Opt. Express **16**, 11987-11994 (2008).
15. F. Blanchard, L. Razzari, H.-C. Bandulet, G. Sharma, R. Morandotti, J.-C. Kieffer, T. Ozaki, M. Reid, H. F. Tiedje, H. K. Haugen, and F. A. Hegmann, "Generation of 1.5 μJ single-cycle terahertz pulses by optical rectification from a large aperture ZnTe crystal," Opt. Express **15**, 13212-13220 (2007).
16. M. D. Thomson, M. Kreß, T. Löffler, and H. G. Roskos, "Broadband THz emission from gas plasmas induced by femtosecond optical pulses: From fundamentals to applications," Laser Photon. Rev. **1**, 349–368 (2007).
17. H. Zhong, N. Karpowicz, and X.-C. Zhang, "Terahertz emission profile from laser-induced air plasma," Appl. Phys Lett. **88**, 261103 (2006).
18. J. Dai and X.-C. Zhang, "Terahertz wave generation from gas plasma using a phase compensator with attosecond phase-control accuracy," Appl. Phys. Lett. **94**, 021117 (2009)

#106703 - $15.00 USD Received 22 Jan 2009; revised 14 Mar 2009; accepted 15 Mar 2009; published 31 Mar 2009

19. W. Liu and S. L. Chin, "Direct measurement of the critical power of femtosecond Ti:sapphire laser pulse in air," Opt. Express **13**, 5750-5755 (2005).
20. S. L. Chin, S. A. Hosseini, W. Liu, Q. Luo, F. Theberge, N. Akozbek, A. Becker, V. P. Kandidov, O. G. Kosareva, and H. Schroeder, "The propagation of powerful femtosecond laser pulses in optical media: physics, applications, and new challenges," Can. J. Phys. **83**, 863-905 (2005).
21. http://www.thzdb.org/
22. B. E. A. Saleh and M. C. Teich, *Fundamentals of photonics* (John Wiley & Suns, Inc. 1991).
23. Q. Wu, M. Litz, and X.-C. Zhang, "Broadband detection capability of ZnTe electro-optic field detectors," Appl. Phys. Lett. **21**, 2924-2926 (1996).

1. Introduction

Terahertz (THz) wave radiation has recently attracted a lot of attention in the scientific community, due to its enormous potentials in probing several (still unexplored) material properties. The THz frequency range (~ 0.1 - 10 THz), which covers the gap between microwaves and infrared light, exhibits distinctive absorptive and dispersive properties for numerous molecules [1-3]. However, there is still a lack of THz pulse sources with high intensity and large bandwidth. Recently, as much as 30 μJ of THz pulse energy was obtained [4] by using 28 mJ of laser input energy and the tilted wave front method [5] in a Lithium Niobate crystal. However, the relatively low peak frequency (0.35 THz) and the associated narrow spectrum (<1 THz) may somehow affect the range of possible applications.

THz radiation generated from laser induced-plasma was first observed in 1993 [6]. More recently, using four-wave mixing [7-10] or ionization induced transient currents in air [11, 12] single-cycle THz pulses with field strengths of the order of hundreds of kV/cm have been reported, based on pump laser intensities of 10^{14}–10^{15} W cm^{-2}. The main advantage of using plasma as the THz generation medium is that unlike any nonlinear crystal, plasma has no thermal damage threshold and can be pumped at extremely high intensities. At the Advanced Laser Light Source (ALLS) laboratory of the Institut National de la Recherche Scientifique (INRS) [13] in Canada, the peak laser intensity of the pump beam can be as high as 10^{20} W cm^{-2} [14] and it is expected to reach even higher intensities of about 10^{23} W cm^{-2} in the near future. Therefore, new THz generation mechanisms that capitalize on relativistic laser-plasma interactions may lead to THz sources with unprecedented power levels and associated performances.

Here we propose a high power, high stability two-color laser-plasma source generating THz radiation. The present paper will study the intensity dependent spatial drift of the emitting plasma, which affects similar sources in their standard configuration, and will propose a simple and straightforward solution to overcome this problem. Our preliminary studies may path the way to new high power and broad-spectrum THz sources with increased stability, and potentially may be a good alternative for high frequency THz generation compared with traditional optical rectification sources based on large aperture ZnTe [15].

2. Experimental

In order to perform our experiments, we used the 80 mJ, 100 Hz, Ti:sapphire beam line of ALLS (800 nm central wavelength) [13]. This line has a beam diameter of 40 mm (at $1/e^2$), a temporal pulse duration of 35 fs and a single pulse energy up to 20 mJ in our case. The experimental setup (see Fig. 1), includes a 100 μm thick beta barium borate (BBO) (type I) crystal placed after either a fused silica lens or a gold off-axis parabolic mirror to generate the second-harmonic (2ν) pulse, which propagates collinearly with the fundamental (ν) pulse. The focal length of the lens and of the off-axis mirror was chosen to be 150 mm in both cases. We varied the polarization and intensity of the 2ν pulse by rotating the ordinary axis of the BBO crystal with respect to the polarization of the incoming fundamental pulse. The relative phase between the ν and 2ν pulse was controlled by adjusting the distance between the BBO crystal and the laser focal spot [11]. The generated plasma was observed from a direction perpendicular to the beam propagation, using a 12-bit Pixelfly CCD camera (640 × 480 pixels,

#106703 - $15.00 USD Received 22 Jan 2009; revised 14 Mar 2009; accepted 15 Mar 2009; published 31 Mar 2009

with a pixel size of 9.9 × 9.9 μm). A 50 mm diameter, 75 mm focal distance off-axis parabolic mirror was placed after the plasma, to collimate both the THz and the plasma-generating beams. To block the ν and 2ν pulses, we placed a 0.5-mm-thick, high resistivity silicon window and two layers of black polyethylene (each ~100 μm thick) in the collimated path. Furthermore, two 100-mm-diameter wire-grid polarizers model G30-L from Microtech Instrument were used to control both the intensity and the polarization of the THz beam.

We detected the THz waves via free-space electro-optic (EO) sampling in a (110) ZnTe crystal with a thickness of 500 μm, by temporally scanning the optical probe with respect to the THz pulse. In addition, the ZnTe detector crystal was mounted onto a mechanical translation stage to maximize the detected THz signal. A lock-in amplifier referenced to the chopper placed after the plasma formation was used to acquire the THz waveforms.

THz energy was measured using a pyroelectric detector (Coherent-Molectron) with a specified sensitivity of 2624 V/J at 1.06 μm, which we previously calibrated at THz frequencies using a second pyroelectric detector from Microtech Instruments based on $LiTaO_3$ crystal [15]. Finally, to further characterize the THz beam, a $BaSrTiO_3$ (BST) pyroelectric infrared camera (Electrophysics, model PV320-L2Z) was used to image the THz beam at the focus. This camera operates with an internal 10 Hz chopper and has a 320 × 240 pixel imaging array with a pixel spacing of 48.5 μm.

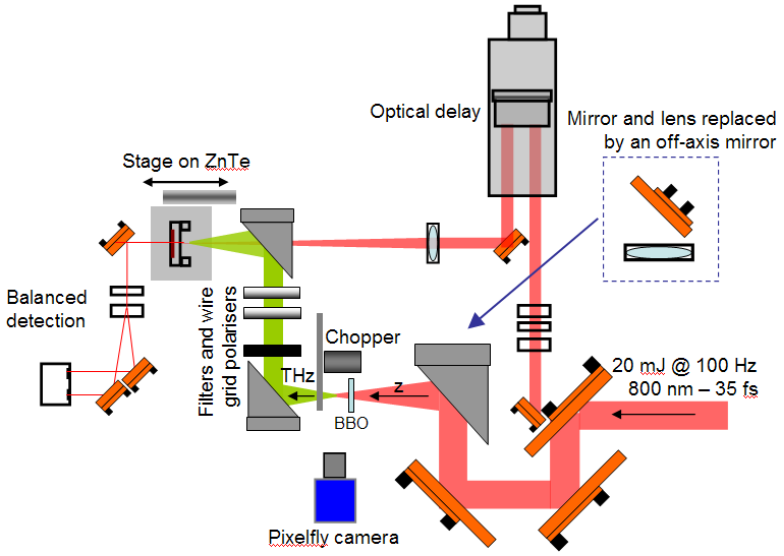

Fig. 1. Schematic of the THz two-color plasma set-up at the Advanced Laser Light Source. A Pixelfly CCD camera was used to visualize the plasma at the focus. The schematic clearly shows the modification we have implemented in order to avoid focal shifting.

3. Results

3.1. Spatial dependence of the focal position

Several groups have investigated the effect of the plasma volume on the conversion efficiency of terahertz generation [16, 17]. M. D. Thomson *et al.* predicted that a larger plasma volume would generate higher efficiency THz radiation [16], while H. Zhong *et al.* emphasized on longer plasma formation for a more directional THz output [17]. Both authors also discussed the importance of the phase walk-off introduced by defocusing inside the plasma, which may decrease or limit the THz conversion efficiency. Recently, this last effect of walk-off was investigated in more detail by J. Dai *et al* [18] who showed further optimization of terahertz emission from gas plasma, by using a phase compensator to control with attosecond precision the relative phase between the 800 nm and 400 nm pump. In this work, we point out a

#106703 - $15.00 USD Received 22 Jan 2009; revised 14 Mar 2009; accepted 15 Mar 2009; published 31 Mar 2009

different effect that may have a significant impact on THz generation when it is obtained via a two-color plasma source when used at high input laser energies (>1 mJ). Namely, the plasma position tends to shift toward the focusing lens, a phenomenon which is observed when we increase the laser input pulse energy and which may affect the measurement of the THz electric field. Such spatial focal shift has been discussed and observed in previous THz work [16] or in specialized report on the generation of filaments by an ultrafast laser beam [19], but without comment on how it affect the THz detection side.

By using a CCD camera placed perpendicularly to the direction of laser propagation (z direction), one can map the overall shift of the focal position as a function of the laser energy. To avoid saturation of the CCD camera and to emphasize the view of the main laser beam/plasma, we used an interference filter centered at 800 nm (10 nm FWHM band-pass). In Fig. 2, we show images of the plasma shifting as a function of the laser input energy for two cases: case A is for plasma generated using a 150 mm focal length lens, and case B is for plasma generated using a gold off-axis parabolic mirror with the same focal length. We noticed that as we increase the laser energy, the plasma generated using an off-axis parabolic mirror shows smaller expansion along the laser propagation direction for the same laser energy, while the width (in the direction perpendicular to laser propagation) tends to expand slightly faster.

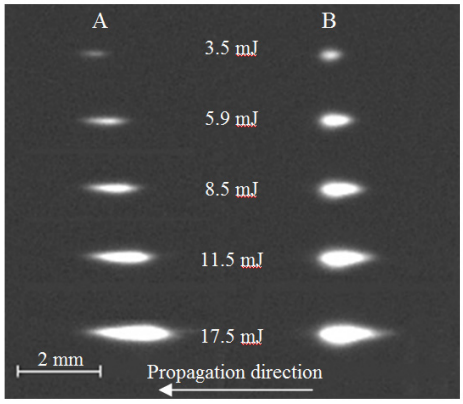

Fig. 2. Image of the plasma generated using a focusing transmission lens (A), and a gold off-axis parabolic mirror (B).

To further emphasize the difference between the two cases presented in Fig. 2, we plot the plasma profile curves in the laser propagation direction. In Fig. 3, we show the plasma intensity profiles as a function of the laser input energy when using a lens (case A) and an off-axis parabolic mirror (case B). Note that the laser propagates from right to left in Fig. 2 and 3.

In case A, one clearly sees that the peak position of the plasma profiles (which also corresponds to the plasma position with the largest vertical dimension) shifts toward the focusing lens and is accelerated as the input laser energy is increased. In particular, this acceleration is significantly higher than the one observed for case B. By looking at the maximum intensity position, a shift toward the lens of more than 1100 μm is observed for case A, while only ~ 120 μm shift is observed for case B. This observation suggests that the THz generated using a lens-based set up will have to travel through a longer plasma section, if we assume a maximum THz emission at the maximum intensity profile position. More details on parameters that affect the plasma formation, such as pulse shape or pulse phase front and self-focusing can be found in [20]. Finally, from Fig. 3 we also notice a different scaling of the plasma induced scattering of the optical pump for the two situations. In case B, the plasma scattering increases faster, but also tends to saturate faster (i.e. at lower laser intensities). In section 3.2, we will expand on these observations and include a discussion on the generated THz radiation.

#106703 - $15.00 USD Received 22 Jan 2009; revised 14 Mar 2009; accepted 15 Mar 2009; published 31 Mar 2009

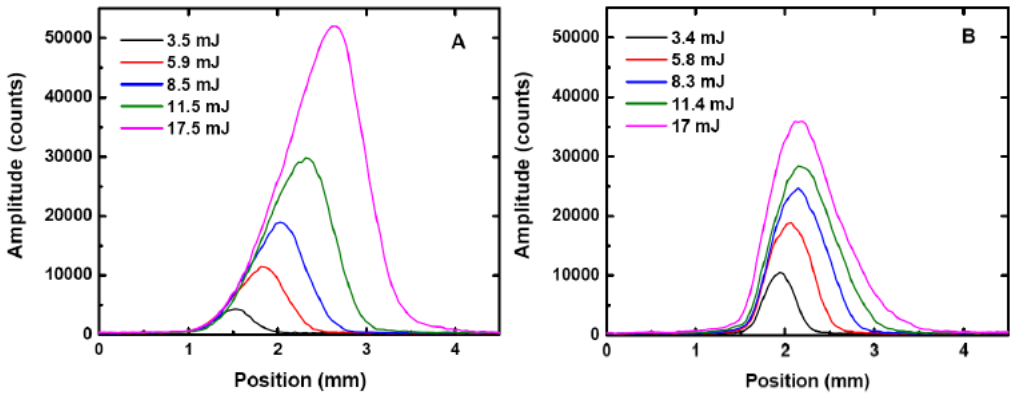

Fig. 3. Axial intensity values of the plasma formation in the propagation direction for: (A) lens focusing and (B) gold off-axis parabolic mirror focusing. Theses images are taken using a 10 nm band-pass filter centered at 800 nm to image the plasma induced scattering of the optical pump.

Based on these plasma images and profiles, we investigated the effect of the shifted focal position on THz detection. A first noticeable consequence of the energy-dependent source shift is the relative displacement (in the direction opposite to laser propagation) of the THz focal spot at the detector position. That is the main THz emission point changes due to the shift in the source position. By scanning the ZnTe detector along the direction of THz propagation (z-profiling), we have mapped the electric field signal for different energies as a function of distance for the two focusing configurations, i.e. for a lens and an off-axis parabolic mirror, respectively. Figure 4 shows the trace of the peak electric field for different input laser energies (note that the THz beam propagates from left to right in these figures). As we increase the input laser energy, we observe a shift in the position of the maximum electric field of more than 4 mm when using a transmission lens, while such a shift is not observed when using an off-axis parabolic mirror.

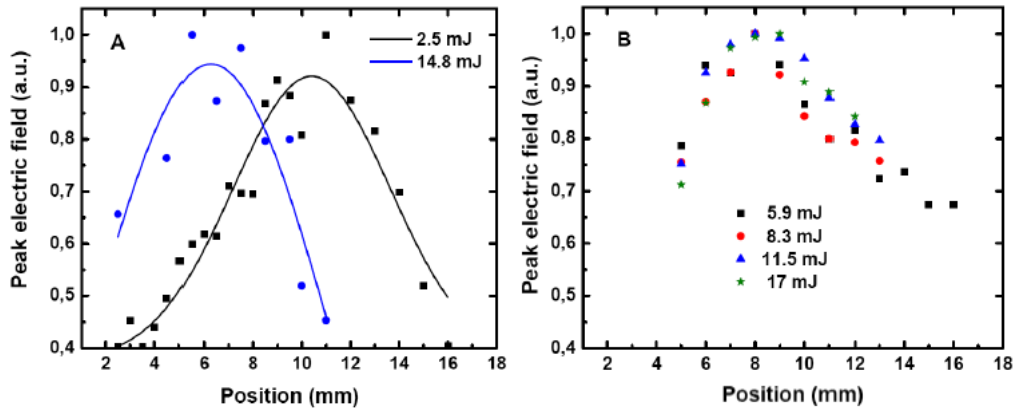

Fig. 4. Peak electric field values as a function of the ZnTe detector position. (A) Normalized peak electric field and Gaussian fit curves obtained from a transmission lens with a 150 mm focal length. (B) Normalized peak electric field measured from a gold off-axis parabolic mirror with the same focal length.

This 4-mm THz shift for the lens case, when compared to the plasma drift of 1.1 mm, indicates that diffraction of the THz beam by the plasma may magnify the overall shift of the THz focus on the detection side. Moreover, it is also possible that the observed shift results from the different THz emission location inside the plasma as the pump energy changes. Incidentally, the shift in the position of the THz beam at focus for high (>10 mJ) and low (<5

#106703 - $15.00 USD Received 22 Jan 2009; revised 14 Mar 2009; accepted 15 Mar 2009; published 31 Mar 2009

mJ) input laser energy may introduce an under-estimation in the measured electric field by more than 30 %. This effect may change the overall behavior of the THz electric field scaling as a function of laser energy, if one does not correct for the ZnTe detector position. Finally, we observed a change in the THz spectra as a function of energy and/or position, which could be attributed to absorption or diffraction of the THz beam within the plasma. This effect needs to be investigated in more detail using simulations, which will be the subject of another paper.

3.2. Measured THz energy

Figure 5 shows the total THz pulse energy generated as a function of the pump energy, which was varied from 1 mJ to 20 mJ. For this measurement, as hinted before, we used two types of filters to eliminate the remaining ν and 2ν pulses: a 0.5 mm thick high resistivity silicon window, together with two layers of black polyethylene. These filters are transparent to THz frequency below 7 THz (defined for a 3 dB cutoff frequency) [21]. The maximum THz signal was obtained by adjusting the distance between the BBO crystal and the focal position, when the ν and 2ν pulses where phase matched. Further, for maximum THz conversion efficiency, the BBO crystal angle was carefully adjusted to be around 55 degrees relatively to the normal optic axis, in good agreement with the configuration already adopted in previous works [12].

At a maximum excitation energy of 20 mJ and by using a gold off-axis parabolic mirror, we obtain a THz pulse energy of 140 nJ per pulse. If we correct our measurement for the Fresnel losses associated to the reflections in the silicon wafer, we obtain a conversion efficiency of 1.7×10^{-5}. In comparison, THz generation using a lens showed a lower conversion efficiency of 6.6×10^{-6} only with a corresponding THz energy of 50 nJ for 15 mJ of pump laser energy.

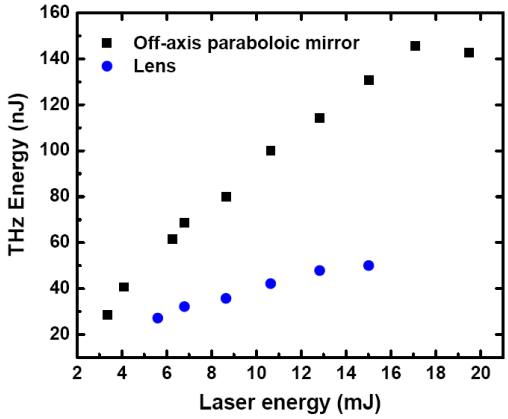

Fig. 5. Total THz pulse energy emitted from a two-color plasma source as a function of the incident 800 nm laser excitation energy, for a lens (diamonds) and a gold off-axis parabolic mirror (squares) . The focal length was 150 mm in both cases

It is interesting to note that the saturation of the THz generation process occurs at a lower pump energy for the lens-focusing configuration. A reason for the higher THz yield when using the off-axis parabolic mirror may be the better superposition between the ν and 2ν pulses.

Generally, one would expect a bone-shaped plasma profile symmetric around the focal region (thus reflecting the region where a plasma threshold is exceeded), and growing with increasing pulse energy. However, in a focusing geometry, the focus will be shifted towards the focusing lens when the laser power exceeds the critical power for self-focusing [19]. Moreover, plasma defocusing will disrupt the bone-like shape after the focus, causing the beam to diverge, resulting in the profiles shown in the present paper.

#106703 - $15.00 USD Received 22 Jan 2009; revised 14 Mar 2009; accepted 15 Mar 2009; published 31 Mar 2009

We observed that the peak plasma position shifts only in the lens configuration (~1.1 mm), while no significant shift is observed in the off-axis parabolic case. Moreover, one finds similarity between the THz profile mappings (in the z direction) in Fig. 4 and the plasma profiles retrieved from Fig. 3. This observation suggests a maximum THz emission from the peak intensity position of the plasma emission, as previously mentioned in section 3.1.

To better understand why this happens, we performed a comparison between the spot sizes generated by the 800 nm laser beam at the focus position. Assuming a Gaussian beam, the following equation gives the spot size for a diffraction-limited beam [22]:

$$2\omega_0 \approx \frac{4}{\pi}\lambda F_{\#}, \tag{1}$$

Where ω_0 is the spot size of the Gaussian beam at focus at which the field amplitude is reduced by a factor 1/e compared to its value on axis, λ is the laser wavelength and $F_{\#}$ is the F-number. Assuming a Gaussian beam of 40 mm diameter and a focal length of 150 mm, one can estimate a diffraction limited spot diameter of ~4 μm in vacuum.

To actually measure the spot size of the 800 nm pump beam for the two focusing configurations, we used the knife-edge technique. A knife is scanned perpendicularly across the beam's axis of propagation, and a photodiode measures the intensity of the unmasked portion of the beam. The measured beam spot sizes at focus are 40 μm and 120 μm ($1/e^2$ of the intensity) for the lens and the off-axis parabolic mirror cases, respectively, which are both much larger than the diffraction-limited spot size. For the lens case, the larger spot size may be due to spherical/achromatic aberration, while for the gold off-axis parabolic mirror, the distorted phase front induced by the mirror surface is probably the dominant factor. In fact, we have noticed a strong diffraction of visible laser light using the gold off-axis parabolic mirror. Note that the surface quality of the 4 inch diameter gold off-axis mirror is $\lambda/2$ at 1 μm wavelength. When using the off-axis parabolic mirror, the relatively large spot size diameter of 120 μm keeps the laser intensity low enough to maintain the maximum peak plasma profile position at the same location, thus allowing a better phase matching between the ν and 2ν pulses.

3.3. THz Spot size evaluation

To rigorously compare the measured THz electric field with the measured THz energy, we first performed an experiment to evaluate the THz spot size. For this, we calculated the THz focal spot size at the detector position by using the Rayleigh range measured in Fig. 4. For Gaussian beam optics, the relation between the Rayleigh range and the beam waist is defined by the following equation:

$$w_I = \sqrt{\frac{Z_R \lambda}{2\pi}}, \tag{2}$$

Here, λ is the THz wavelength, w_I is the THz spot size at focus (1/e value of the intensity profile) and Z_R is the Rayleigh range. As a result, we obtained a waist of 420 μm when using a lens, and 400 μm when using an off-axis parabolic mirror (i.e. comparable within the experimental error).

Next, we actually imaged the THz focus, using a $BaSrTiO_3$ (BST) pyroelectric infrared camera. The results for both the off-axis and the lens case are shown in Fig. 6. From these images, one can extract a THz beam waist (w_I) of 120 μm for both cases. The smaller THz spot size obtained using the camera may be explained by the non-negligible contribution of the high-frequency components generated during this process. For example, in reference [12] the authors reported THz signal detected up to 75 THz, which is only limited by the chosen detection technique. Such high-frequency components cannot be detected by the ZnTe electro-optic detector [23], but can pass through the filters (silicon window, black

#106703 - $15.00 USD Received 22 Jan 2009; revised 14 Mar 2009; accepted 15 Mar 2009; published 31 Mar 2009

polyethylene with a 3 dB bandwidth at 7 THz and wire grid polarizers) and are thus detected by the pyroelectric camera, which is calibrated and responds linearly from 0.6 to 20 μm. Moreover, one cannot completely attenuate the THz image seen by the pyroelectric camera by cross polarizing the two G30-L wire grid polarizers (Microtech Instrument, contrast higher than 100:1 for frequencies below 3 THz). This also indicates that a non-negligible portion of the signal recorded by the pyroelectric detector lies between 3 to 20 THz (since the black polyethylene passes these frequencies, while being opaque to visible light), but is outside of the frequency bandwidth of the ZnTe detector. Therefore, one should be especially careful when comparing the electric field with the energy reading.

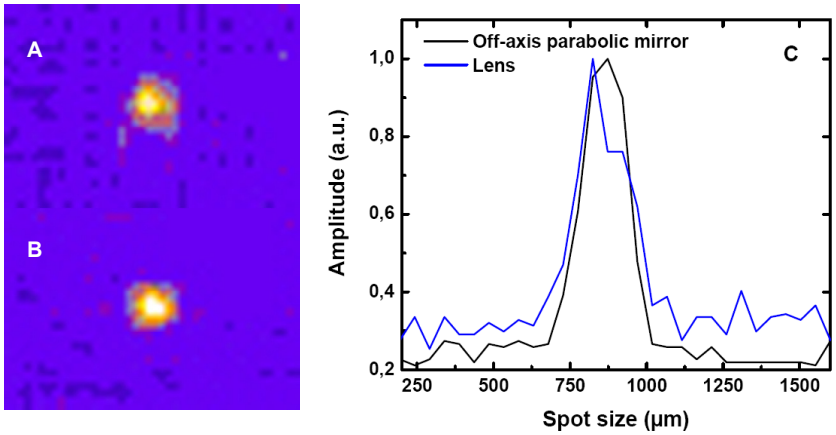

Fig. 6. Real time image of focused THz pulse obtained with an infrared pyroelectric camera (ElectroPhysics model PV320-L2Z). THz spot images obtained for (A) a two-color plasma source using lens based focusing; (B) a two-color plasma source using a gold off-axis parabolic mirror based focusing. (C) In-line profiles extracted from the THz images.

3.4. Measured THz electric field

There have been recently several reports on high THz electric field generation using plasma based THz sources [9-12]. The largest THz electric field reported to date is as high as 400 kV/cm with an estimated THz pulse energy of 30 nJ [9], and it has been achieved using a pump laser with 0.5 mJ energy and 25 fs pulses duration. Other groups, using laser energies lower than 1 mJ, but with longer pulses width, have measured THz electric fields on the order of 10 kV/cm [11,12]. More recent results demonstrate THz electric fields higher than 150 kV/cm [11], obtained with 20 mJ of input laser energy and 50 fs pulses duration.

In this study, we adopt a method for evaluating the THz electric field that is similar to that reported in [16], by using a formula derived directly from Maxwell's equations:

$$E_0 = \sqrt{\frac{\eta_0 W}{\pi w_I^2 \int g^2(t)dt}}, \tag{3}$$

Here, E_0 is the THz peak electric field, η_0 is the free space impedance (377 Ω), W is the THz energy, w_I is the intensity beam waist obtained from equation (2) and $g(t)$ is the temporal shape of the THz electric field (with peak value normalized to 1), which can be easily retrieved from the EO sampling measurements.

Since we use a ZnTe crystal to characterize the electric field, the associated bandwidth was limited to ~3 THz, while the energy measured using the pyroelectric detector could span the full bandwidth of the two-color plasma source [12], and was only restricted by the 3 dB cutoff at 7 THz induced by the black polyethylene filter [21]. To estimate the THz electric field red by the EO sampling in ZnTe, we adopt the same assumption as in [16], i.e. we have divided the THz energy measured by the pyroelectric detector by a factor of 2. Using Eq. (3),

#106703 - $15.00 USD Received 22 Jan 2009; revised 14 Mar 2009; accepted 15 Mar 2009; published 31 Mar 2009

the electric field estimated for the lens case obtained with 15 mJ of pump laser energy is 70 kV/cm. For the same laser excitation, the use of an off-axis parabolic results in an estimated THz electric field of 125 kV/cm.

It is important to note that we performed these measurements in a non-purged environment with >40% relative humidity, which led to a significant ringing of the THz electric field due to water absorption (see Fig. 7). Moreover, high electric field measurements for the configuration with an off-axis mirror suggest an "over rotation" when a 0.5-mm thick ZnTe crystal detector is used. This over-rotation will in turn lead to under-estimating the actual electric field, since the detector crystal does not respond linearly in that range of high electric field measurements. To avoid this situation and to reduce the THz intensity inside the ZnTe detector, we used the two wire-grid polarizers. Finally, by retrieving the THz waveform by the EO sampling, one can estimate the electric field using equation (3).

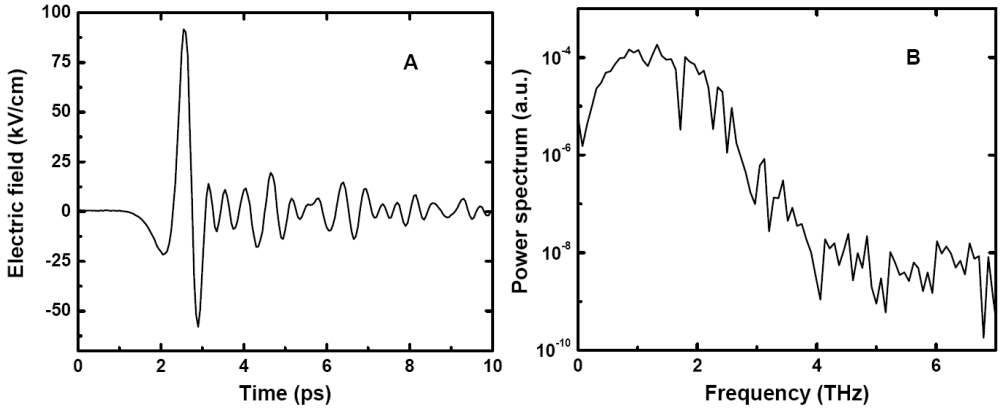

Fig. 7. (A) Electric field plot obtained with the off-axis parabolic mirror configuration using 9 mJ of laser excitation. (B) Power Fourier transform of the electric field plot.

4. Conclusions

In conclusion, we have demonstrated and characterized a two-color plasma THz pulse source using two different focusing configurations. This study has shown how the THz electro-optic sampling technique is affected by the source drifting, when a lens is used to promote plasma formation. We showed that a way to avoid this intensity-dependent shift is by replacing the lens with a gold off-axis parabolic mirror. Incidentally, this configuration resulted in a >2 times increase in THz generation efficiency when compared to the lens configuration case. The full physical parameters that are involved during the plasma formation are still under investigation. Finally, we have performed a full evaluation of the generated THz electric field, by combining information on the THz spot size and the EO sampling detector response in function of the z coordinate.

Acknowledgments

We wish to acknowledge financial support from *le Fonds Québécois de la Recherche sur la Nature et les Technologies* (FQRNT) and the *Natural Sciences and Engineering Research Council of Canada* (NSERC) and V. Bartulovic at Novacam LTD for supporting this work. L. Razzari wishes to acknowledge a Marie Curie Outgoing International Fellowship (contract n. 040514). We are also thankful to Antoine Laramée and François Poitras for their technical assistance with the ALLS laser source.

#106703 - $15.00 USD Received 22 Jan 2009; revised 14 Mar 2009; accepted 15 Mar 2009; published 31 Mar 2009